

# Numerical Modelling of Light Emission and Propagation in (Organic) LEDs with the Green's Tensor

Horst Greiner\*

Philips Research Laboratories, Aachen

Olivier J.F. Martin\*\*

Ecole Polytechnique Fédérale de Lausanne

## Abstract

The accepted model for light emission and propagation in organic LEDs (OLED) which consists of several optically thin functional layers deposited on a thick substrate is a classical dipole located in the emitting layer. The propagation of the emitted light is commonly described by a Fourier expansion of the dipole field into plane waves which represent the various radiating and bound modes of the layered structure in  $k$ -space. To calculate the electric and magnetic fields inside and outside the LED an integration over the individual plane waves has to be performed. This entails numerical difficulties which can be overcome elegantly with the so-called Green's tensor approach for stratified media recently developed by the second author. In our contribution we demonstrate the applicability of this method to the computation of electromagnetic field distributions in organic LED structures. Visualizations of typical field distributions arising from individual dipoles are presented and discussed thus allowing a more intuitive understanding of effects relating to dipole location and orientation and material absorption. Furthermore it is shown that scattering of bound modes by particle like inhomogeneities of the layer structure can be effectively modelled with the Green's tensor approach. Visualizations are presented and discussed with regard to increased light extraction.

**Keywords:** numerical modelling, organic light emitting diodes, light emission, light extraction, dipole radiation, stratified media, layered media, Green's tensor

## 1. Introduction

Improved light extraction is a key factor for increasing the efficiency of solid state light sources available on the market today. Their lumen efficiency already surpasses incandescent sources by a factor of 2 and with further improvements light emitting diodes could become a real competitor for fluorescent lamps in the near future. But even in state of the art devices the major part of the internally generated photons remains trapped in the device: extraction efficiencies vary between 10 to 50%, depending on the device structure and the emitted wavelength. For an overview on light extraction techniques from inorganic light emitting diodes we recommend chapter 5 in <sup>1</sup>. Organic light emitting diodes are described in <sup>2,3</sup>. For a review of light extraction from organic LEDs see <sup>4,5,6,7</sup>.

The basic reason for light being trapped in the device is the high refractive index of the light emitting, cladding and substrate layers <sup>6,7</sup>: for inorganic LEDs this index can reach values well above 3 whereas for organic LEDs it can go up to 2. Light emitted into these layers is then caught by total internal reflection at the interfaces between the high and low index media and can only escape to the outside world through narrow angular cones perpendicular to the chip surfaces. Simple considerations show that this is the case for only a fraction of about  $1/n^2$  of the generated photons, where  $n$  is the index of refraction of the emitting medium. In the framework of this simple geometrical optics model, light extraction can be modelled quite accurately by raytracing techniques assuming isotropic emission, particularly for inorganic LEDs and light trapping by thin film solar cells <sup>8</sup>.

\* [horst.greiner@philips.com](mailto:horst.greiner@philips.com) phone +49-241-6003-435 fax +49-241-6003-483, Philips Forschungslaboratorien GmbH, Weisschausstr.2, 52066 Aachen, Germany

\*\* [olivier.martin@epfl.ch](mailto:olivier.martin@epfl.ch) phone +41-21-6932607 fax +41-21-6932614, Metrology and photonics laboratory, STI-ITOP-MET, ELG 240, 1015 Lausanne EPFL, Switzerland

For more advanced designs like Resonant Cavity LEDs,<sup>9</sup> where the emitting layer is surrounded by several optically thin layers, this simple model is no longer valid as interference effects have to be taken into account. All the more this applies to organic LEDs which consist basically of a light emitting layer with a thickness of a few hundred nanometers sandwiched between two metal electrodes of comparable dimensions<sup>2</sup>, one of which is transparent, the whole stack being deposited on a thick glass substrate. The full Maxwell equations have to be solved for a stratified medium made up by the various layers for a dipole radiator located in the emitting layer in order to describe light emission and propagation in such devices correctly. This classical problem of mathematical physics<sup>17</sup> was already tackled in the beginning of the last century by Hermann Weyl and Arnold Sommerfeld, who gave solutions in terms of analytically defined integrals with highly oscillating integrands which numerical evaluation proves to be difficult. In a more mathematical language the problem amounts to solving the Helmholtz wave equation in a layered medium with arbitrary permittivities (including absorbing and anisotropic media) for each layer, the right hand side being given by a delta function describing the pointlike dipole source. As a matter of fact this is a standard problem in mathematical physics, which solution is given as explained in the following sections by the Green's tensor if we take the vectorial nature of the fields into account. Providing another instance of "the unreasonable effectiveness of mathematics in the natural sciences"<sup>11</sup> the Green's tensor and the plane wave expansion associated with it contains all the physics of the problem like the existence of guided modes and plasmon-polariton modes arising from the metal electrodes<sup>13, 14</sup>. Knowledge of the Green's tensor also allows to compute the spontaneous emission rate of the dipole in the framework of quantum electrodynamics. Compared to other established methods of solving the Maxwell equations for the emission problem in layered media like the Finite DifferenceTime Domain or modal methods, the Green's tensor makes the physical problem more transparent and tractable. Furthermore the method is not restricted to lossless and isotropic but can also deal with absorbing and anisotropic media.<sup>16</sup> A further advantage of the Green's tensor approach is the possibility to model light scattering by particle-like inclusions in the layers, including photonic band gap structures to enhance light outcoupling<sup>15, 18</sup>. But one has to keep in mind that light extracted from the thin layers into the thick glass substrate can still be caught by total internal reflection at the glass/air interface. This can be mitigated by microstructuring this surface<sup>10</sup>.

In this contribution we would like to attract the attention of the reader to a numerically very efficient and reliable way of calculating the Green's tensor<sup>19</sup> and demonstrate how it can be used to model light emission and propagation in organic light emitting diodes. In this way we want to help to fulfil "The promise of solid state lighting for General Illumination" as advocated in the OIDA/DOE report<sup>12</sup> where quantitative modelling for optimization of light emitting diodes is strongly recommended to progress towards higher lumen efficiencies of solid state light sources.

The paper is organized as follows: in section 2 we introduce the Green's tensor and outline an efficient numerical scheme for its computation developed a few years ago by the second author and co-workers. We then discuss how it can be used to model scattering structures included in the layers and how the computational load of these calculations can be greatly reduced by exploiting the rotational and translational symmetries of the problem.

Section 3 starts with some general considerations of light emission and propagation in organic LEDs. Visualizations of the Poynting vector fields describing energy flow in typical OLEDs are presented. We then give some examples of scattering calculations performed for single and small arrays of cylinders or spheres of subwavelength dimensions and present some intriguing pictures of the energy flows arising from the scattering.

The conclusion points out directions for further work also in comparison to other approaches to describe light outcoupling by biperiodic grating structures, our aim being to establish a comprehensive quantitative model for light extraction from OLEDs.

## 2. Modelling Light emission and propagation in stratified media

In this section we explain how the Helmholtz wave equation can be solved for a dipole emitter embedded in a layered medium by the Green's tensor. Only the bare outlines can be given, for more details the reader should consult the references<sup>19, 20, 21, 22, 23, 24</sup>.

### 2.1 The Green's tensor approach to dipole emission in layered media

The presentation follows<sup>17, 19</sup>. Consider a radiating dipole with dipole moment  $\mathbf{p}$  embedded in a medium of constant permittivity  $\epsilon$  at location  $\mathbf{r}'$ . Its electrical field

$$\mathbf{E}(\mathbf{r}, t) = \mathbf{E}(\mathbf{r})e^{-i\omega t} \quad (2.1.1)$$

is then given by the Helmholtz equation

$$\nabla \times \nabla \times \mathbf{E}(\mathbf{r}) - k_B^2 \epsilon_B \mathbf{E}(\mathbf{r}) = \mathbf{p} \delta(\mathbf{r} - \mathbf{r}'). \quad (2.1.2)$$

$\epsilon_B$  denotes the permittivity of the medium and  $k_B^2 = \omega^2 \epsilon_B$  and  $\delta$  the Dirac function. It is well known that the solution of this equation is

$$\mathbf{E}(\mathbf{r}) = \mathbf{G}(\mathbf{r}, \mathbf{r}') \cdot \mathbf{p}, \quad (2.1.3)$$

where the 3x3 Green's tensor is specified by

$$\mathbf{G}(\mathbf{r}, \mathbf{r}') = \left( \mathbf{I} + \frac{ik_B R - 1}{k_B^2 R^2} \mathbf{I} + \frac{3 - 3ik_B R - k_B^2 R^2}{k_B^2 R^4} \mathbf{R}\mathbf{R} \right) \frac{\exp(ik_B R)}{4\pi R} \quad \text{with } \mathbf{R} = \mathbf{r} - \mathbf{r}' \quad (2.1.4)$$

The Green's tensor contains both a near and a far field component (for an interesting discussion with visualizations see <sup>25</sup>).

Let us now consider a layered medium where the permittivity is a piecewise constant function of  $z$  but does not depend on  $x$  and  $y$ . We assume that there are only a finite number of layers bounded from above and below by infinite media of constant permittivity and that the dipole is embedded in one of the layers. To obtain a solution of the Helmholtz equation, i.e. the Green's tensor for the layered medium, we observe that the electromagnetic fields from the dipole are scattered at the layer interfaces. To account for this we consider the plane wave expansion of the form

$$G_{ij}(\mathbf{r}, \mathbf{r}') = \frac{i}{8\pi^2} \iint \frac{1}{k_z} \left[ \delta_{ij} - \frac{k_i k_j}{k_B^2} \right] \exp(ik_x(x - x') + ik_y(y - y') + ik_z|z - z'|) dk_x dk_y \quad (2.1.5)$$

The indices  $i$  and  $j$  can take the values  $x, y$  and  $z$  and

$$k_z = \text{sign}(z - z') \sqrt{k_B^2 - k_x^2 - k_y^2}. \quad (2.1.6)$$

For  $i=j=z$  there is an additional term

$$-\frac{1}{k_B^2} \delta(\mathbf{r} - \mathbf{r}'). \quad (2.1.7)$$

We can now match these plane waves in each layer  $l$  with corresponding up and down going plane waves of the form

$$A_{ij}^{\pm}(k_z) \exp(ik_x(x - x') + ik_y(y - y') \pm ik_z(z - z')) \quad (2.1.8)$$

with

$$k_z = \sqrt{k_1^2 - k_x^2 - k_y^2} \quad k_1^2 = \omega^2 \epsilon_1 \quad (2.1.9)$$

to solve the source free Helmholtz equations. By the standard matching procedure for the electric and magnetic fields at the layer boundaries the matrix coefficients  $A_{ij}$  can be obtained for each layer as rational algebraic functions of  $k_z$  using a standard recursive procedure. In this way a plane wave representation  $\mathbf{G}_l$  of the Green's function of the layered medium is obtained in each layer  $l$  including the emitting layer.

The real space Green's function is then given by integration of the plane waves. In cylindrical coordinates  $(\rho, \phi, z)$  the integration can be reduced to the evaluation of the so called Sommerfeld integrals whose integrands are given by products of rational algebraic functions and highly oscillating Bessel functions. The efficient numerical evaluation of these Sommerfeld integrals requires sophisticated numerical techniques<sup>19, 26, 27</sup> which description is beyond the scope of this paper. With these numerical integration techniques fast and reliable evaluation routines for the Green's tensor can be constructed. On a modern PC with a processor speed of 1.6Ghz one evaluation of the Green's tensor takes about 50msec.<sup>19</sup>

The power  $W$  radiated by the dipole source  $\mathbf{p}$  into the layered structure can also be readily evaluated from the Green's tensor<sup>14</sup>: from electromagnetic theory it is given by

$$W = 0.5 \omega \text{Im} \mathbf{p}^* \cdot \mathbf{E}(\mathbf{r}_{\text{dip}}) = 0.5 \omega \text{Im} \mathbf{p}^* \cdot \mathbf{G}(\mathbf{r}_{\text{dip}}, \mathbf{r}_{\text{dip}}) \cdot \mathbf{p} \quad (2.1.10)$$

If the Green's tensor is decomposed in a "direct" and "reflected" contribution  $\mathbf{G} = \mathbf{G}_D + \mathbf{G}_R$  arising from the scattering at the layer boundaries we obtain

$$W = 0.5 \omega \text{Im} \mathbf{p}^* \cdot \mathbf{G}_D(\mathbf{r}_{\text{dip}}, \mathbf{r}_{\text{dip}}) \cdot \mathbf{p} + 0.5 \omega \text{Im} \mathbf{p}^* \cdot \mathbf{G}_R(\mathbf{r}_{\text{dip}}, \mathbf{r}_{\text{dip}}) \cdot \mathbf{p} \quad (2.1.11)$$

This shows that the power radiated by the dipole (which gives its quantum mechanical decay rate) is strongly influenced by its layered environment.

## 2.2 Modelling of scattering structures for light outcoupling

One possibility to enhance light outcoupling from organic LEDs is the incorporation of scattering structures into the layers, to tap the guided and plasmonic modes<sup>6, 15, 18, 22, 33, 32</sup>. To be effective the permittivity of these structures should differ from the permittivity of the layer they are embedded in. One can think of small spheres or cylinders arranged in a periodic fashion to produce photonic bandgap effects preventing the propagation of guided modes. Or of simple particles for scattering the energy caught in the plasmonic modes. In this section we want to show how the Green's tensor for the stratified medium describing the organic light emitting diode gives a very effective means to perform such calculations<sup>21, 23, 24</sup>.

Consider small particle like inclusions in the layered medium like shown in fig. 4 and let  $\Delta\epsilon(\mathbf{r}) = \epsilon_1$  if  $\mathbf{r}$  is located in layer  $l$  and  $\Delta\epsilon(\mathbf{r}) = \epsilon_p - \epsilon_1$  if  $\mathbf{r}$  is located in particle  $p$  and layer  $l$ .

Let  $\mathbf{E}^{\text{dip}}(\mathbf{r})$  denote the field produced by the dipole. The total field  $\mathbf{E}(\mathbf{r})$  can then be obtained from the integral equation

$$\mathbf{E}(\mathbf{r}) = \mathbf{E}^{\text{dip}}(\mathbf{r}) + \int_{\substack{\text{scatter} \\ \text{volume}}} d\mathbf{r}' \mathbf{G}(\mathbf{r}, \mathbf{r}') k_0^2 \Delta\epsilon(\mathbf{r}') \mathbf{E}(\mathbf{r}'), \quad (2.2.1)$$

where  $\mathbf{G}$  is the Green's tensor of the stratified background introduced in the previous section. This integral equation looks deceptively simple. Unfortunately it is not at all obvious how to treat the singularity of the Greens function in the integrand for  $\mathbf{r}=\mathbf{r}'$ . The usual procedure is to apply some averaging of the Green's tensor in a small volume around the singularity to keep the integral meaningful.<sup>22</sup>

Remarkably the integration extends only across the volume of the scatterers which facilitates the solution considerably. Other methods need to discretize the whole domain under consideration and introduce artificial boundary conditions to limit its extension. A further advantage is that the total field is already determined by the values it takes on the scattering volumes and therefore one needs to solve the integral equation only inside the scattering volume. In the exterior the electrical field can be obtained by direct integration.

To solve the integral equation numerically one subdivides the scattering volumes into elementary scattering volumes  $V_i$  centered around locations  $\mathbf{r}_i$  which linear dimensions should be in the order of  $\lambda/10\sqrt{|\Delta\epsilon|}$ , where  $\lambda$  is the free space wavelength of the dipole. The discretization then gives a linear system of equations of the form

$$\mathbf{E}_i = \mathbf{E}_i^{\text{dip}} + \sum_{\text{sites } j \neq i} \mathbf{G}(\mathbf{r}_i, \mathbf{r}_j) k_0^2 V_j \Delta\epsilon(\mathbf{r}_j) \mathbf{E}_j + \mathbf{S}_i \Delta\epsilon(\mathbf{r}_i) \mathbf{E}_i. \quad (2.2.2)$$

The matrix  $\mathbf{S}_i$  describes the averaging performed on the singular volume and is given by a multiple of the identity matrix<sup>23</sup>. Depending on the size and number of the particles employed, this gives a dense linear system of the form  $\mathbf{Ax}=\mathbf{y}$  with thousands of variables. Such systems can be solved efficiently by iterative methods<sup>28</sup> which require the efficient evaluation of the matrix vector product  $\mathbf{Ax}$ . For a system with  $10^4$  scattering sites for instance we would have to evaluate the Green's tensor  $10^8$  times which at the rate of ten evaluations per second would take several thousand hours and require many GB of storage. Fortunately there is a simple way to overcome this obstacle, as described in the next section.

### 2.3 Reducing the number of Green's tensor evaluations for a given problem

In the following we explain how to reduce in a very considerable way the number of evaluations of the Green's tensor for a given problem with or without scattering: Assume for instance we want to calculate Poynting vector field describing the energy flow arising from a single dipole. Then one first has to calculate the electric and magnetic field in the points of interest and then form their vector cross product. If we want to compute the field distribution on a dense grid of points  $\mathbf{r}_i = (x_i, y_i, z)$   $i = 1, \dots, n$  in a horizontal plane given by  $z=\text{const}$  caused by a dipole source

located at  $\mathbf{r}_s = (x_s, y_s, z_s)$ , we have to evaluate the Green's tensor  $\mathbf{G}(\mathbf{r}_i, \mathbf{r}_s)$   $i = 1, \dots, n$ .

If  $n$  is in the order of millions (grids with 1000 by 1000 points) this would require a long computation time even if one evaluation only took a fraction of a second on a fast personal computer. Fortunately this computational load can be decreased by orders of magnitude by exploiting the translational symmetry in the  $x$ - $y$  plane and the rotational symmetry around the  $z$ -axis of the layered medium which are inherited by the Green's tensor:

$$\mathbf{G}(\mathbf{r}_i, \mathbf{r}_s) = \mathbf{G}(x_i, y_i, z_i, x_s, y_s, z_s) = \mathbf{G}(0, 0, z_i, x_s - x_i, y_s - y_i, z_s) \quad (2.3.1)$$

by translational symmetry. Defining the horizontal distance between  $\mathbf{r}_i$  and  $\mathbf{r}_s$  by

$$R_i = \sqrt{(x_i - x_s)^2 + (y_i - y_s)^2} \quad (2.3.2)$$

and exploiting the rotational symmetry around the  $z$ -axis, we obtain

$$\mathbf{G}(\mathbf{r}_i, \mathbf{r}_s) = \mathbf{D}_\theta \mathbf{G}(0, 0, z_i, R_i, 0, z_s) \mathbf{D}_{-\theta} \quad (2.3.3)$$

where

$$\mathbf{D}_\theta = \begin{bmatrix} \cos\theta & -\sin\theta & 0 \\ \sin\theta & \cos\theta & 0 \\ 0 & 0 & 1 \end{bmatrix} \quad \text{with} \quad \cos\theta = \frac{x_i - x_s}{R} \quad \text{and} \quad \sin\theta = \frac{y_i - y_s}{R}$$

Hence by precomputing the Green's tensor  $\mathbf{G}(0,0,z_i, \mathbf{R}, 0, z_s)$  as a function of  $R$  in closely spaced intervals (say 1nm) in the range  $\min R_i \dots \max R_i$  and storing the values in core memory ( only  $G_{11}, G_{22}, G_{33}, G_{31}$  and  $G_{13}$  being not zero), one can easily obtain  $\mathbf{G}(\mathbf{r}_i, \mathbf{r}_s)$  from (2.3.2) and (2.3.3) by linearly interpolating between two neighbouring distance values. If we consider for instance a regular grid with 1000 by 1000 20nm grid cells we have to perform about 30000 Green's tensor evaluations instead of one million!

Clearly this approach also applies to the case when all field points are located on one horizontal plane and all dipole sources on another horizontal plane. If we subdivide the scattering structures such that the elementary scattering volumes are all arranged in distinct horizontal planes, the matrix elements appearing in the integral equation can all be precomputed for each combination of planes. The advantage of this is twofold: firstly not all the matrix elements have to be stored (thus allowing systems with many elementary scattering volumes) and secondly the matrix vector products needed to solve (2.2.2) iteratively can be calculated easily on the fly if the volumes are arranged plane by plane. This enables the application of iterative linear solvers also for complicated systems.

### 3. Model calculations and examples

In this section we apply the Green's tensor to the emission and propagation of light in organic LEDs. The first part treats LEDs without scattering particles and offers visualizations of the power flow in a typical OLED. The following part gives some examples of the effect of scattering on light outcoupling.

#### 3.1 Modelling Light Propagation in unperturbed media

The plane wave spectrum of the dipole with moment  $\mathbf{p}$  describes how the power radiated by the dipole is shared by the radiating, leaky and guided modes. The power going into a particular plane wave  $(k_x, k_y)$  can be obtained from the formula (cf. (2.1.11))

$$W(k_x, k_y) = 0.5\omega \text{Im} \mathbf{p}^* \cdot \hat{\mathbf{G}}_D(k_x, k_y) \cdot \mathbf{p} + 0.5\omega \text{Im} \mathbf{p}^* \cdot \hat{\mathbf{G}}_R(k_x, k_y) \cdot \mathbf{p}. \quad (3.1.1)$$

$\hat{\mathbf{G}}_D$  denote the plane wave spectrum of the direct part and  $\hat{\mathbf{G}}_R$  of the reflected part given in (2.1.5) and (2.1.8) By averaging the dipole positions and performing the respective integrals numerically, one can evaluate the power carried by the various modes and the angular spectrum of the dipole radiation escaping from the device. For examples we refer to the publications<sup>29,30</sup>. To obtain the field distributions in the device<sup>31</sup> one needs to evaluate the full Green's tensor. Here we take an example from<sup>4</sup>: We consider an OLED on a glass substrate ( $n=1.55$ ), covered by the following layers (from bottom to top): ito ( $d=160\text{nm}, n=1.85+0.04i$ ), emissive organic layer ( $d=72\text{nm}, n=2.0$ ) and an optically thick metal cathode ( $n=0.18+i2.35$ ). The emitting dipole is situated 40nm below the metal cathode and radiates at a wavelength of 550nm. Figures 1-3 show the directions and magnitude of the Poynting vector fields in the  $x$ - $z$  plane on a logarithmic scale for the the  $x$  dipole (lying horizontally in the plane), the  $y$  dipole (pointing out of the plane) and  $z$  dipole (pointing upwards). One clearly recognizes the plasmonic modes at the interface of the organic layer and the metal cathode and the waveguiding in the organic and ito layer. The values of the power flowing through the upper and lower interfaces of the organic layer and into the glass have been calculated for the different dipole orientations: for the vertical dipole orientation about two times more energy goes into the metal cathode than for the horizontal one and about three times more "horizontal" than "vertical" light reaches the glass substrate.

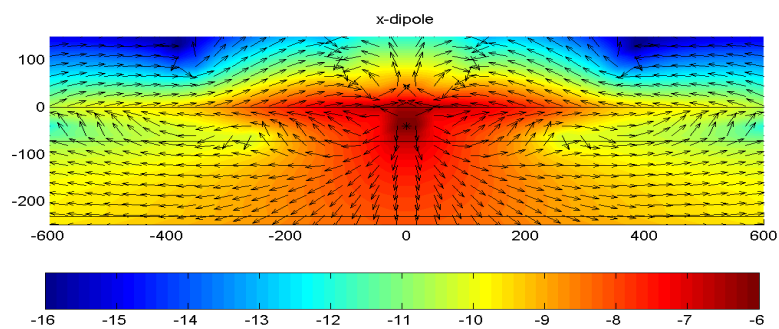


Fig. 1: Poynting vector field in the  $(x,z)$  plane through the dipole. the arrows give the direction and the shading the magnitude on logarithmic scale. The dipole is oriented in the  $x$  direction

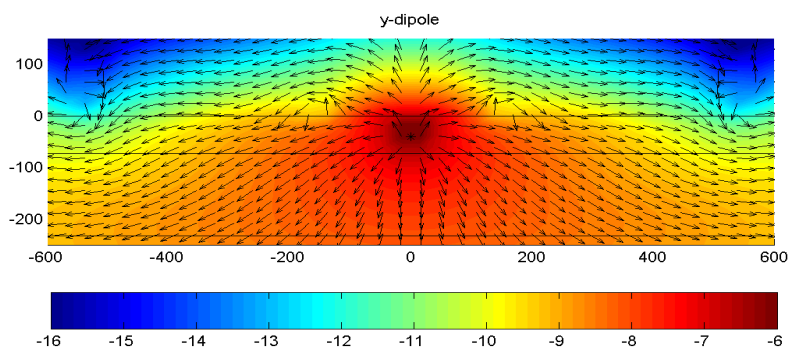


Fig. 2: Poynting vector field in the  $(x,z)$  plane through the dipole. The arrows give the direction and the shading the magnitude on logarithmic scale. The dipole is oriented in the  $y$  direction

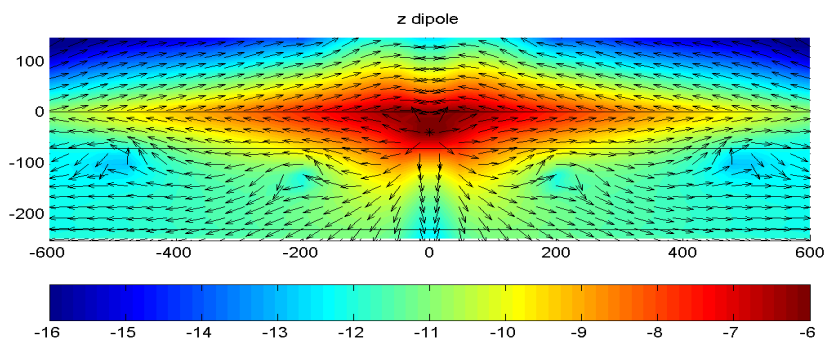


Fig. 3: Poynting vector field in the  $(x,z)$  plane through the dipole. the arrows give the direction and the shading the magnitude on logarithmic scale. The dipole is oriented in the  $z$  direction

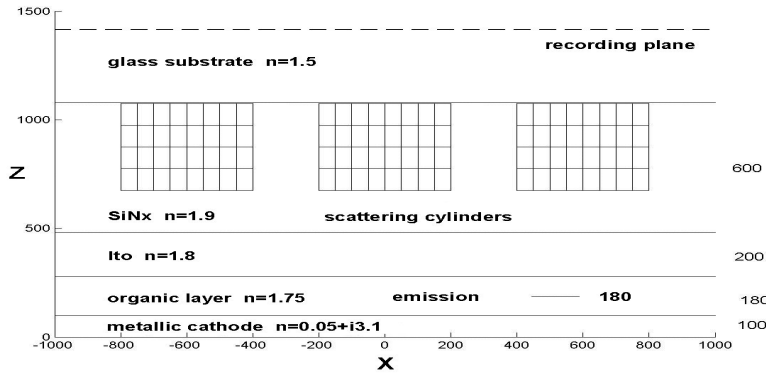


Fig. 4: configuration used for scattering calculations

### 3.2 Scattering by single particles and arrays

In this section we apply the formalism described in section 2.2 and 2.3 to the scattering of the electromagnetic field of a dipole emitter by small cylindrical or spherical inclusions in an organic LED. We have chosen the structure described in<sup>15</sup> and depicted in Fig.4. The cylinders are assumed to have the refractive index of the glass substrate and are surrounded by the SiN<sub>x</sub> layer with n=1.9. They have a radius of 200nm and a height of 400nm. For the spheres we assume the same data, a radius of 200nm and the z location of the centre at 700nm. We have investigated the scattering by small quadratic arrays of cylinders and spheres with one mesh measuring 600 by 600nm. To obtain the subdivision of the scatterers into small volumes, they were surrounded by a tight fitting rectangular box. The enclosing box was then subdivided into 25 by 25 by 25 small boxes of equal size and shape. The scatterer volume was then represented by the boxes which center belonged to it.

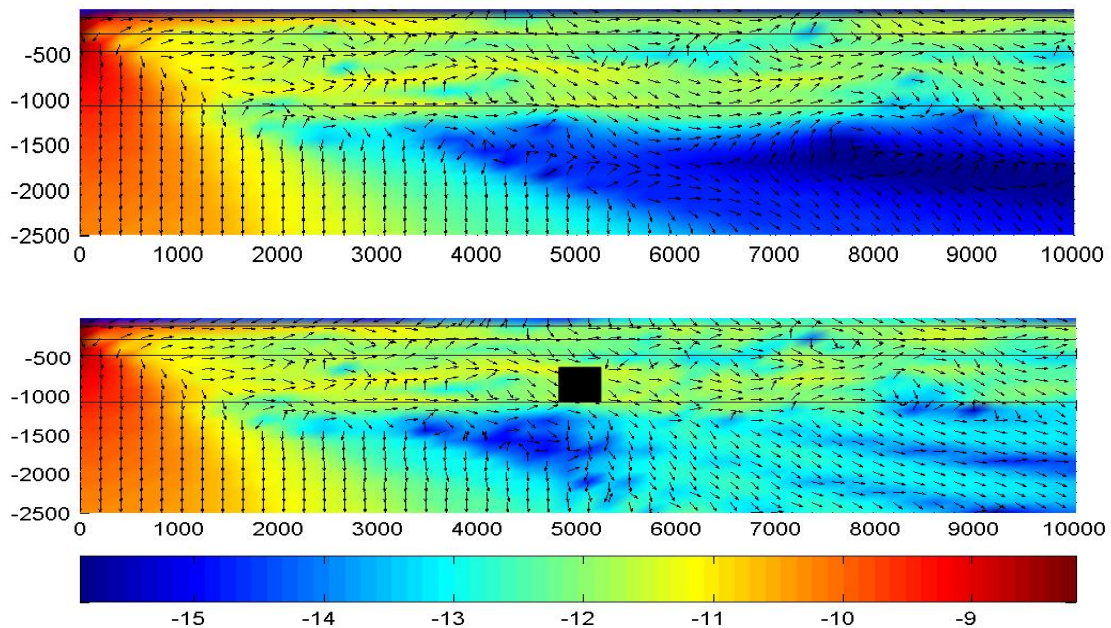


Fig. 5: Scattering of the radiation of a x dipole by a cylinder depicted in black in the lower picture. For comparison the upper picture shows the unscattered radiation. Location of the dipole at x=0, y=0 and z=-180. The arrows give the direction and the false colours the logarithm of the magnitude of the Poynting vector. Glass is at the bottom!



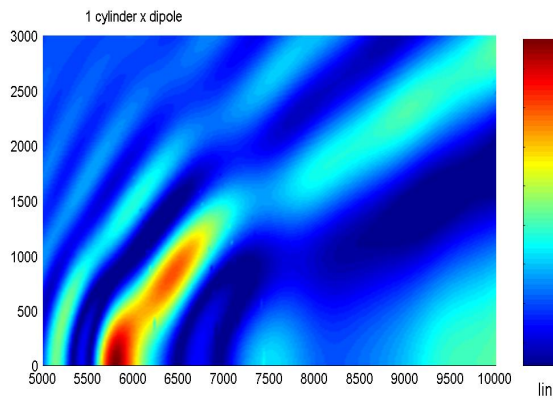


Fig.6: scattering of x dipole from single cylinder in xy-plane at  $z=2000$ .

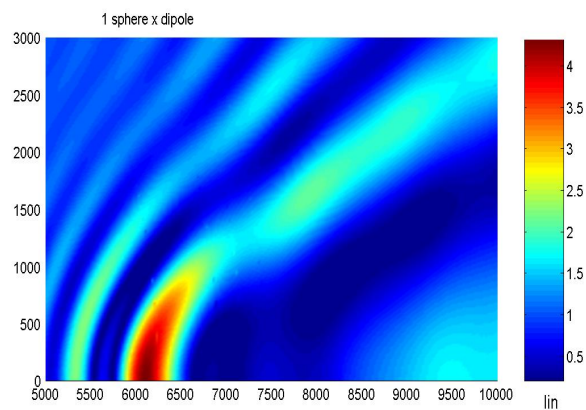


Fig.7: scattering of x dipole from single sphere in xy-plane at  $z=2000$

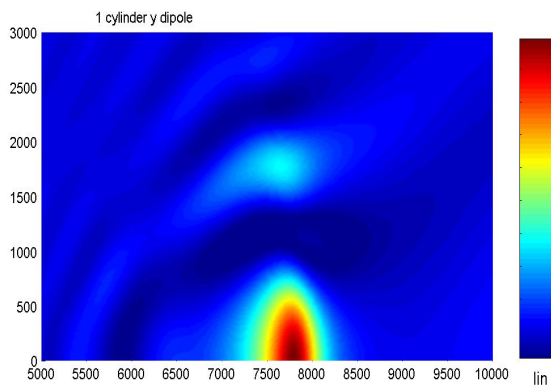


Fig. 8: scattering of y dipole from single cylinder in xy-plane at  $z=2000$

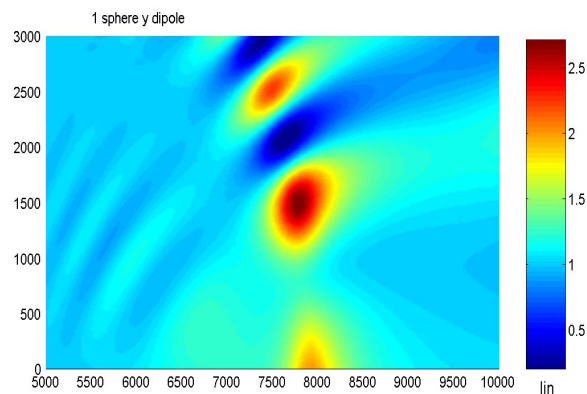


Fig.9: scattering of y dipole from single sphere in xy-plane at  $z=2000$  .

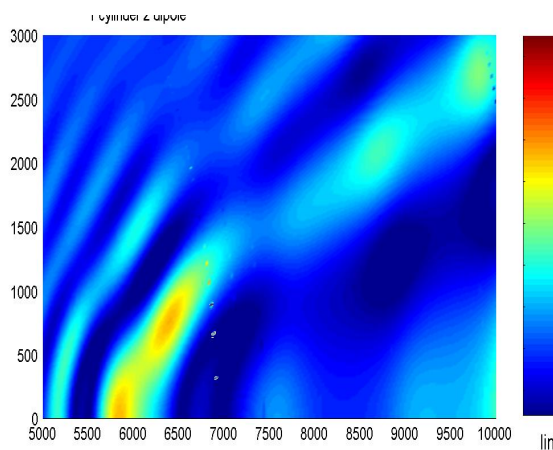


Fig. 10: scattering of z dipole from single cylinder in xy-plane at  $z=2000\text{nm}$

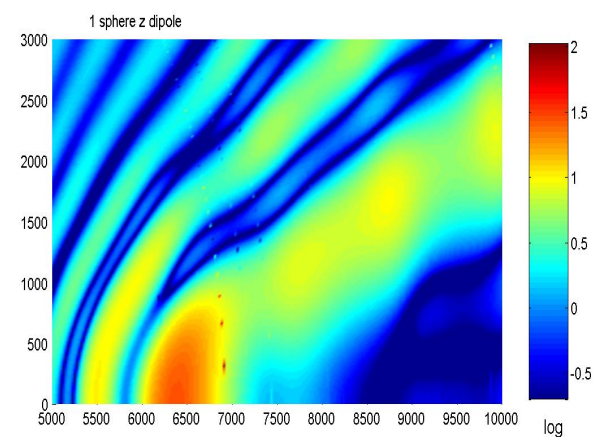


Fig. 11: scattering of z dipole from single sphere in xy-plane at  $z=2000\text{nm}$

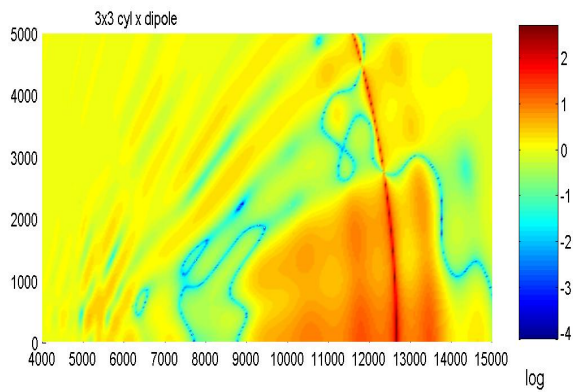


Fig 12: scattering of x-dipole by a 3 by 3 array of cylinders in xy-plane at z=2000nm

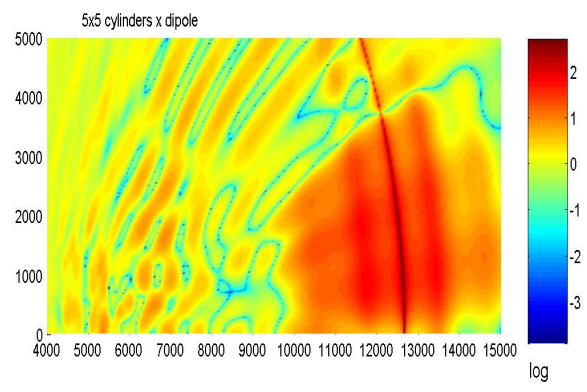


Fig. 13: scattering of a x dipole by a 5 by 5 array of cylinders in xy-plane at z=2000nm

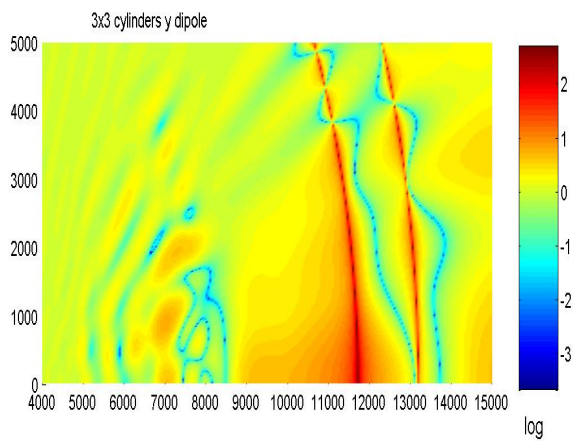


Fig. 14: scattering of y dipole by a 3 by 3 array of cylinders in xy-plane at z=2000nm

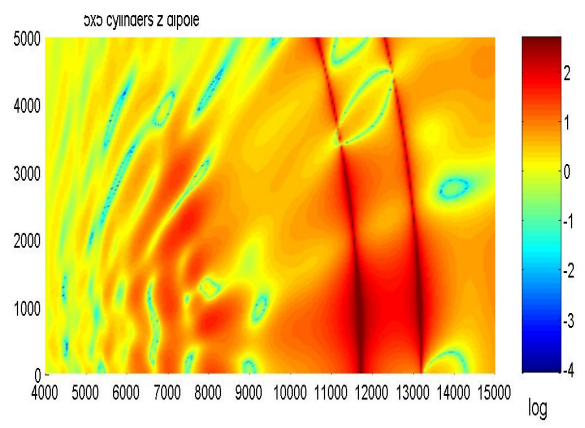


Fig. 15: scattering of y dipole by a 5 by 5 array of cylinders in xy-plane at z=2000nm

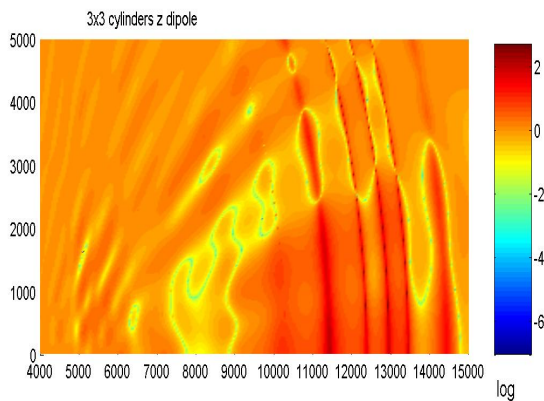


Fig. 16: scattering of z dipole by a 3 by 3 array of cylinders in xy-plane at z=2000nm

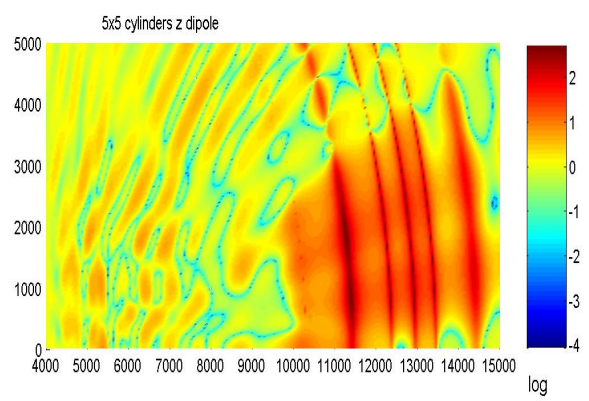


Fig. 17: scattering of z dipole by a 5 by 5 array of cylinders in xy-plane at z=2000nm

According to the results presented in<sup>15</sup> these structures should be effective scatterers. In the following we assume that the “centre” of the scattering structures is located at  $x=5000\text{nm}$  and the emitting dipole at  $x=0\text{nm}$  and  $y=180\text{nm}$ . In this way we ensure that most of the light seen by the scattering structures only consists of leaky or bound modes. In our computational experiments we have calculated the energy flow through a horizontal plane situated in the glass substrate above the cylinders at  $z=2000\text{nm}$ . The normal of the Poynting vector was normalized with regard to the normal of the Poynting vector arising from the same configuration without scattering. This local “outcoupling” factor is displayed in the figures as a function of  $x$  and  $y$  either on a linear or logarithmic scale as appropriate.

In a first series of experiments we have computed the scattering by a single cylinder or sphere for the various dipole orientations ( $x, y, z$ ) (Figs. 5 –11). It is noticeable that the pattern of the scattered light and the integrated outcoupling factor strongly depends on the shape of the scatterer (cylinder or sphere) and the dipole orientation.

In a second series of experiments we have considered scattering by 3 by 3 and 5 by 5 arrays of spheres and cylinders. Some representative results are shown in Figs.12-17. We find the occurrence of lines with very high and low outcoupling factors most remarkable. This should be compared with the results obtained for periodic infinite arrays in<sup>33, 32</sup>.

## Conclusion

We have demonstrated that with an efficient numerical implementation of the Green’s tensor and some pedestrian tricks to reduce the number of Green’s tensor evaluations for a given problem, light propagation and scattering by arrays or clusters of particles in organic LEDs can be effectively modelled. Pertinent examples were presented using the electrical Green’s tensor. To model very large arrays or clusters of particles special methods of numerical linear algebra<sup>28</sup> to solve the integral equations could be investigated.

To assess the outcoupling efficiency of a scattering structure for a given device one clearly would have to average the incoherent contributions of the dipoles with regard to position, orientation and wavelength. This is certainly not possible in a brute force way with the present approach and more sophisticated schemes using a periodic approximation are called for<sup>33</sup>. Nevertheless we believe that our “atomistic” description can help to gain some understanding of the basic scattering mechanisms for improved light outcoupling.

## References

1. A. Zukauskas, M. Shur, R. Caska, *Introduction to Solid-State Lighting*, John Wiley, 2002, chapter 5.
2. J.Shinar, editor, “Organic Light-Emitting Devices”, Springer, 2003
3. N.K. Patel, S.Cina, J.H. Burroughes, “High Efficiency Organic Light-Emitting Diodes”, IEEE Journal on Selected Topics in Quantum Electronics, Vol.8, no.2, 346-361, 2000
4. J.A.E. Wasey, A.Safonov, I.D.W. Samuel, W.L. Barnes, “Efficiency of radiative emission from thin films of a light-emitting conjugated polymer”, Physical Review B, Volume 64, 205201, 2001
5. K.Meerholz, D.C. Müller, “Outsmarting Waveguide Losses in Thin-Film Light-Emitting Diodes, Advanced Functional Materials, vol.11, no 4, p.251-53, 2001
6. W.L. Barnes, “Electromagnetic Crystals for Surface Plasmon Polaritons and the Extraction of Light from Emissive Devices”, Journal of Lightwave Technology, vol. 17, no 11, 2170-2182, 1999
7. M.-H. Lu, J.C. Sturm, “External coupling efficiency in planar organic light-emitting devices”, Applied Physics Letters, Vol 78, no 13, 1927-1929, 2001
8. R. Brendel, “Thin-Film Crystalline Silicon Solar Cells”, Wiley-VCH, 2003
9. D. Delbeke, R.Bockstaele, P. Bienstman, R. Baets, H. Benisty, “ High-Efficiency Semiconductor Resonant-Cavity Light-Emitting Diodes: A Review”, IEEE Journal on selected Topics in Quantum Electronics, Vol 8, No 2, 189-206, 2002
10. C.F. Madigan, M.-H. Lu, J.C. Sturm, “Improvement of output coupling efficiency of organic light-emitting diodes by backside substrate modification”, Applied Physics Letters, Vol 76, no 13, 1650-1652, 2000
11. E. Wigner, “The Unreasonable Effectiveness of Mathematics in the Natural Sciences”, Communications in Pure and Applied Mathematics, vol 13, no 1, 1960

12. OIDA/DOE report, "The Promise of Solid State Lighting for General Illumination", [http://www.eren.doe.gov/buildings/documents/pdfs/oida\\_led-oled\\_rpt.pdf](http://www.eren.doe.gov/buildings/documents/pdfs/oida_led-oled_rpt.pdf), Optoelectronics Industry Development Association, Washington, DC, March 2001
13. M.S. Tomas, "Green function for multilayers: Light scattering in planar cavities", *Physical Review A*, vol 51, no 3, 2545-2559, 1995
14. M.S. Tomas, "Damping of a dipole in planar microcavities", *Optics Communications*, vol 100, no 1,2,3,4, 259-267, 1993
15. Y.J. Lee, S.Kim, J.Huh, G.H. Kim, Y.H.Lee, "A high-extraction-efficiency nanopatterned organic light-emitting diode", *Applied Physics Letters*, Vol.82, no.21, 3779-3781, 2003
16. F. Olyslager, I.V. Lindell, "Green's Dyadics for Bianisotropic Media", *Review of Radio Science 1999-2002*, Editor W. R. Stone, IEEE Press, John Wiley&Sons, 2002
17. J.A. Kong, "Electromagnetic Wave Theory", EMW Publishing, Cambridge Mass 2000, chapter 6.6
18. T. Yamasaki, K.Sumiooka, T.Tsutsui, "Organic light-emitting device with an ordered monolayer of silica microspheres as a scattering medium", *Applied Physics Letters*, Vol 76, no 10, 1243-1245, 2000
19. - M. Paulus, P. Gay\_Balmaz, O.J.F. Martin, "Accurate and efficient computation of the Green's tensor for stratified media", *Physical Review E*, vol 62 no 4, 5797, 2000
20. M. Paulus, O.J.F. Martin, "Light propagation and scattering in stratified media: a Green's tensor approach", *J.Opt.Soc.Am. A*, Vol. 18, No.4, 854-861, 2001
21. M. Paulus, O.J.F. Martin, "A fully vectorial technique for scattering and propagation in three-dimensional stratified photonic structures", *Optical and Quantum Electronics* 33, 315-325, 2001
22. M. Paulus, O.J.F. Martin, "How to tap an innocent waveguide", *Optics Express*, Vol.8, No.12, 644-648, 2001
23. O.J.F. Martin, N.B. Piller, "Electromagnetic scattering in polarizable backgrounds", *Physical Review E*, Vol.58, No. 3, 3909-3915, 1998
24. M. Paulus, O.J.F. Martin, "Green's tensor technique for scattering in two-dimensional stratified media", *Physical Review E*, volume 63, 066615, 2001
25. T. Setälä, M. Kaivola, a.T. Friberg, "Decomposition of the point-dipole field into homogeneous and evanescent parts", *Physical Review E*, Vol 59, no 1, 1200-1206, 1999
26. W. Cai, T. Yu, "Fast Calculations of Dyadic Green's Functions for Electromagnetic Scattering in a Multilayered Medium", *Journal of Computational Physics*, vol 165, 1-21, 2000
27. T.J. Cui, W.C. Chew, "Fast evaluation of Sommerfeld Integrals for EM Scattering and Radiation by Three-Dimensional Buried Objects", *IEEE Transactions On Geoscience AND Remote Sensing*, Vol. 37, No 2, 887-900, 1999
28. U. van Rienen, "Numerical Methods in Computational Electrodynamics, Linear Systems in Practical Applications", Springer 2001
29. K.A. Neyts, "Simulation of light emission from thin-film microcavities", *J.Opt.Soc.Am.A*, vol 15, no 4, 962-971, 1998
30. K.A. Neyts, P. De Visschere, D.K. Fork, G.B. Anderson, "Semitransparent metal or distributed Bragg reflector for wide-viewing-angle organic light-emitting-diode microcavities", *J.Opt.Soc. Am.B.*, vol 17, no 1, 114-119, 2000
31. K.B. Kahen, "Rigorous optical modelling of multilayer organic light-emitting diode devices", *Applied Physics Letters*, Vol.78, no 12, 1649-1651, 2001
32. H. Rigneault, F. Lemarchand, A. Sentenac, H. Giovannini, "Extraction of light from sources located inside waveguide grating structures", *Optics Letters*, Vol. 24, No 3, p.148-150, 1999
33. D. Delbeke, P.Bienstman, R.Bockstaele, R.Baets, "Rigorous electromagnetic analysis of dipole emission in periodically corrugated layers: the grating-assisted resonant cavity light-emitting diode", *J.Opt.Soc.Am. A*, vol.19, no 5, 871-880, 2002